JOURNAL OF COMPUTATIONAL PHYSICS 5, 587–611 (1970)

Numerical Methods of Some Transsonic Aerodynamics Problems

O. M. BELOTSERKOVSKII

Computing Center of the Academy of Sciences of the USSR, Moscow, USSR

Received January 9, 1970

In this paper a short review of the numerical methods used for the determination of the aerodynamic characteristics of high-speed vehicles with transsonic and supersonic velocities will be given. Generally we will be concerned with steady problems of external aerodynamics for blunt bodies.

I. INTRODUCTION

1. In recent years much attention has been paid to the study of transsonic problems of gas dynamics including vorticity. Such problems arise, for instance, in the flow past bodies with a detached shock wave, in the flow past a discontinuity point of the body surface, on wings in super-critical flow, in nozzles, and so on. Aerodynamic and stability characteristics in these regimes have not been studied sufficiently.

In transsonic regions complex mixed gas flows take place, and so-called "floating" shocks and local supersonic zones may develop. The difficulties of such problems are related to the complicated mathematics (boundary layer problems for non-linear elliptic-hyperbolic equations of motion of a compressible rotational gas). It should be noted that most analytical investigations are devoted to the study of plane potential transsonic flows, therefore new approaches had to be developed to deal with rotational and mixed flows in three dimensions.

Only numerical methods using high speed computers and careful experiments allow us to get the complete solution to the above problems and to determine the necessary flow characteristics. Thus, the elaboration of numerical schemes, the calculation of different transsonic gas dynamics problems, as well as the study of analytical properties of the solutions and their asymptotic behavior are of significant interest at present.

2. The numerical schemes were developed under our supervision and collaboration in the Moscow Physical Technical Institute and the Computing Center of the Academy of Sciences of the USSR. The work was done by young scientists, post-graduates or undergraduates.

The review given is not claimed to be a complete account of the field. We shall simply draw the reader's attention to some peculiarities of the numerical schemes and the methods of solving steady gas dynamics problems presently being used. We shall mention the new results obtained recently and discuss the problems of the development and use of the numerical algorithms for carrying out serial calculations in solving modern engineering problems arising in practice.

II. Numerical Method Survey

1. *Steady-State Schemes*

In determining the steady aerodynamic characteristics of bodies (especially when electronic computers of average power were employed) we made wide use of the following methods for solving steady gas dynamics equations, the method of integral relations (m.i.r.), the method of characteristics (m.ch.) and some finite difference schemes (e.g., schemes with "artificial viscosity", and others). We wish to consider especially problems in which different discontinuities and singularities are given beforehand, together with some associated boundary conditions; the solutions being carried out in regions where functions vary continuously.

As is known, three different schemes of the method of integral relations were developed for the determination of flow in the region of a blunt nose, namely, using an approximation for the initial functions across the shock layer (Scheme I), along it (Scheme II) or in both directions (Scheme III). As a result the boundary value problem was solved for an approximate system of ordinary differential (algebraic) equations. To solve the three dimensional problems, some additional trigonometric approximation in the circumferential coordinate was introduced [1, 2]. For different flow conditions and different body shapes one of the schemes of the method of integral relations has been found applicable; they are widely used in our country as well as abroad.

The main advantage of these schemes is that, by means of different transformations, one succeeds eventually in approximating functions (or groups of functions) with comparatively weak variations. It allows us to obtain reliable results and a high degree of accuracy with a comparatively small number of interpolation nodes (usually 3–4 calculated points were used).

The choice of the independent variables, the form of the initial system of equations of motion (that is, the introduction of the integrals into the initial system, the use of the divergent form of the laws of conservation and others), the use of conservation schemes, the approximation of the integrals, etc., are all of great importance in writing the numerical algorithm using m.i.r., and hence in producing results.

The main difficulty in carrying out the schemes of m.i.r. is the solution of many parameter boundary problems for the approximating system of equations. This was overcome by means of different iteration schemes. Moreover, these schemes were used in transsonic regions mainly for bodies of a comparatively simple form, while when dealing with a supersonic zone one had to adopt another algorithm.

In calculating supersonic flow the two- and three-dimensional schemes of the method of characteristics by P. I. Chushkin, K. M. Magomedov, and their coworkers were used [3, 4]. As is known, having written down the initial form of the system in characteristic variables, one requires approximation of ordinary derivatives only. Using a fixed linear computational network, we get a system of finite difference equations with its several advantages.

With the help of the above mentioned approaches, a large number of gas dynamics problems have been solved, namely, ideal gas flows with chemical reactions and radiation, transsonic and three-dimensional flows, as well as viscous flows. In most cases sufficiently steady and reliable results were obtained, which were in perfect agreement with experiment. However, these approaches to the solution of the steady-state equation may be successfully used only for problems in which there are no singularities, discontinuities, intersections, and interactions. The application of these approaches is difficult for bodies of complex form with a large number of discontinuities. Besides, a single algorithm for the calculation of different types of flow is preferable.

2. *Unsteady-State Schemes*

The next step in the evolution of numerical methods, which was motivated by urgent practical needs and aided by the availability of electronic computers, was the development of nonsteady schemes and the use of the stability method for the solution of steady-state aerodynamic problems. We tried to keep to the general principles and ideas of the m.i.r. and m.ch. in approximating the nonsteady equations with respect to space variables. The divergent or characteristic form of the initial equations were used, the same calculations networks were employed, etc.

In this way the nonsteady Schemes II and III of the method of integral relations and the network-characteristic method were developed [5]. These allow us to consider rather complicated types of flow with a single algorithm. It is natural that the problems of stability and the attainment of steady-state solutions should become crucial. They require some specific technique such as the introduction of artificial viscosity into the initial system, and of dissipation terms into the difference equations. In a number of cases the accuracy of the results obtained is less than in the steady-state methods, but these approaches enabled us to consider new classes of problems; for example, the determination of the aerodynamic character-

istics of three-dimensional flow for specific configurations, the calculations of viscous transsonic flows, and others.

3. *"Large Particles" Method*

Finally, in the third stage of development it seemed reasonable and advantageous to introduce the elements of the Harlow "particle-in-cell" method [6] into the algorithms. At first only the equation of continuity is represented as the mass flow across the Euler cell, using the simplest finite difference or integral approximation along the coordinates.

Thus the modified method of "large particles" [7, 8] came into existence, which (again by means of the stability process) allowed us to consider from one point of view such a complicated task as, for example, the subsonic, transsonic, and supersonic flow past a flat nosed body in two dimensions or with axial symmetry. Such an approach is used in calculating viscous flows, and it may permit us to study the characteristics of separated flows.

Thus, this review is concerned with the development of a definite class of numerical schemes used for the estimation of the aerodynamic characteristics of vehicles. It should be stressed that the development of the numerical schemes mentioned above is determined by the improvement and extension of the ways of solving the boundary value problems for the corresponding approximating equations; by the consideration of a new, wider class of problems; by the development and improvement of the electronic computers, machine languages, input and output arrangements, and so on. At the same time the algorithms are made according to principles of the method of integral relations, the method of characteristics, and other approaches. We shall not dwell on these methods in this paper, as the details are described in the articles referred to.

III. Results of The Calculations

The problems of flow past bodies at small free-stream supersonic velocities, and of the singularities of the flow around bodies with sonic discontinuities (solved by means of m.i.r. and m.ch.) are considered in succession. The calculations of the flow around a cylindrical body under supersonic and transsonic conditions (the large-particles method) and three-dimensional flows are also examined. In conclusion, some properties of flows with floating shocks are studied.

1. *Flows Around Bodies at Small Supersonic Velocities*

The investigation of properties of flows around bodies at small supersonic velocities is of considerable interest. With a decrease in the Mach number of the oncoming flow, the region of influence of the mixed flow is markedly increased.

While investigating this problem we should take into consideration the transsonic character of the flow between the sonic line and the limiting characteristic bounding the minimum region of influence of the blunt nose. Disturbances in the transsonic region will affect the form of the sonic line, and, consequently, the whole flow in the mixed zone. The solution of the boundary value problem becomes more dependent on the change of initial data, the errors due to approximations increase, and the calculation becomes unstable. All this requires the construction of special numerical schemes. It is essential to know the boundaries of various types of minimum regions of influence of the blunt nose.

The most effective method in the case is Scheme III of the method of integral relations [1, 2] in which the representation of functions in two directions is used,

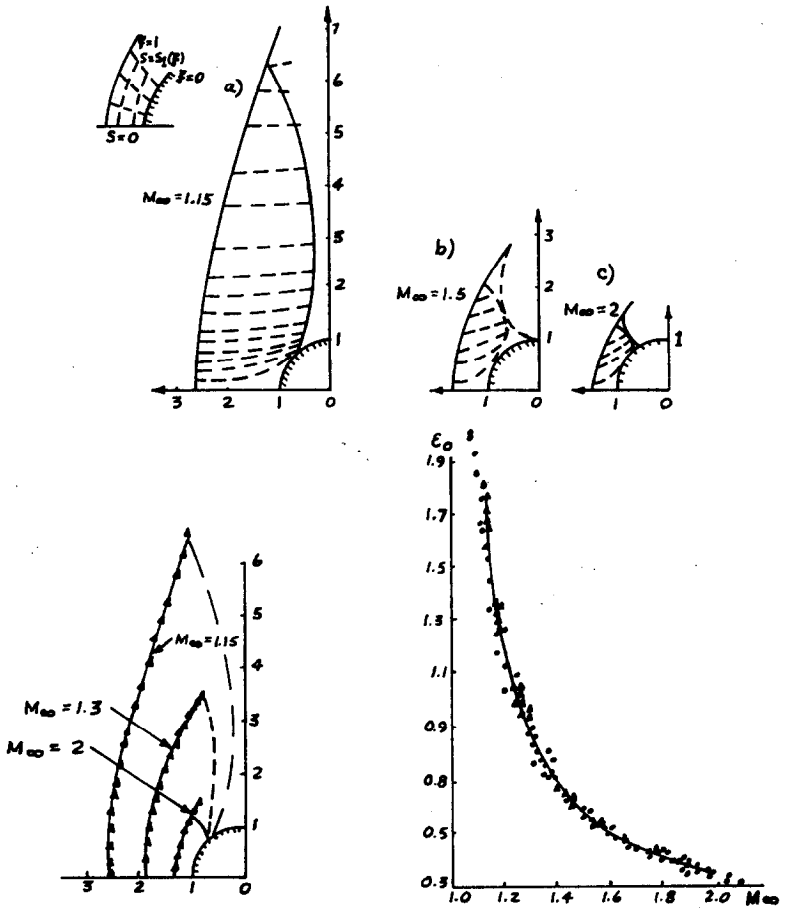

FIGURE 1

and the initial equations are approximated by a nonlinear system of algebraic equations on a curvilinear computational net (Fig. 1). By means of these schemes, F. D. Popov [2] succeeded in carrying out calculations up to a Mach number of the undisturbed flow of $M_\infty = 1.05$. Besides, a complete system of equations of gas dynamics including vorticity was considered in this case. The calculation of sonic flow ($M_\infty = 1$, potential flow), when the shock wave is detached from the body at an infinite distance, was performed by P. J. Chushkin, also by means of the method of integral relations [9]. Fig 1 shows some of the results obtained. The positions and forms of shock waves, sonic lines, streamlines, and limiting characteristics of the first and second families at different values of M_∞ are given.

As can be seen, with a decrease of Mach number the flow pattern is markedly changed. The sonic line departs sharply from the axis of symmetry, turning downstream near the sonic point, the position of this point being slightly dependent on M_∞. The region of influence of the blunt nose is restricted to two characteristics of different families tangential to the sonic line (II type). With a decrease of the undisturbed velocity far upstream, the point of tangency is displaced towards the shock wave. The main changes in gasdynamic quantities are confined to the vicinity of the surface of the body. The large curvature of the streamline is observed also only in the immediate neighborhood of the body. It is noteworthy that the given type of minimum region of influence exists for flow around a sphere up to $M_\infty = 1.1$.

In the same Figure a comparison is shown between the calculation by F. D. Popov and experimental data by V. G. Maslennikov, A. P. Bedin, G. J. Mishin, et al. on the detachment distance of the shock wave along the axis of symmetry (ϵ_0), as well as on the form and position of the waves. It is seen that the agreement between calculation and experimental data is extremely good. The tables of flow fields for the given flow conditions are presented in a monograph [2].

2. *Singularities of Flow Around Bodies With A Sonic Discontinuity*

The calculation of supersonic flow around bodies with a discontinuity in the slope of the contour is of great practical value since the presence of a sharp corner on the body, for a given radius of curvature of bluntness, decreases the heat exchange near the stagnation point.

In the case where we introduce a jump in slope of the contour, the flow pattern is changed, so that the local sonic velocity of the flow may be attained at the point of discontinuity (sonic discontinuity), the calculation of such flows is considerably complicated by the presence of a singularity. The zone of expansion of flow around the corner will be in a region of mixed transsonic flow accompanied by a sharp change of velocity, both in magnitude and direction. In addition, in the supersonic flow zone near the surface of the body a "floating" shock may occur, which considerably affects the whole flow pattern. It is noteworthy that the

results of calculation of mixed flows in the region of influence of the blunt nose provide further initial data for the calculations in the supersonic zone. The calculation for bodies with a break of contour in the transsonic zone must be made with a high degree of accuracy, since even small errors in the computation prevent us from continuing the calculation into the supersonic zone. For the calculation of such flows Scheme I or Scheme II of the method of integral relations were used [1, 2].

In the first scheme the above method was applied both in the region ahead of the corner and in the supersonic expansion around it, where the initial equations are given in a polar system of coordinates with origin at the corner. The system of ordinary differential equations is integrated numerically along the shock layer from the axis of symmetry. In the vicinity of a corner (where the Prandtl–Meyer solution is valid) a differential relation is used, which is the condition of compatibility along a characteristic of the second family.

In the second case, by means of the construction of limiting characteristics, it is possible to separate out exactly the region of influence of the blunt body, which clearly improves the accuracy of the computations in every approximation. Here, in the vicinity of the corner (region G), we use the asymptotic solution of Vaglio–Laurin–Shugayev in a form convenient for our calculations [2] (Fig. 2).

$$(1)\quad \boxed{\begin{array}{ll} U = 1 + (\varkappa+1)^{-1/3}\sum_{i=0}^{\infty}\tilde{u}_i(\zeta)\,\bar{n}^{(2+i)/4} & V = \sum_{i=0}^{\infty}\tilde{v}_i(\zeta)\bar{n}^{(3+i)/4} \\ \zeta = (\varkappa+1)^{-1/3}\bar{S}\,\bar{n}^{-5/4} & \bar{n} = n/r_0^* \qquad \bar{S} = (S-S_*)/r_0^* \end{array}}$$

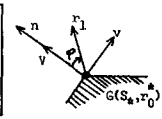

$$i = 0 \qquad \tilde{u}_0 = g' \qquad \tilde{v}_0 = (7g - 5\zeta g')/4$$

$$(2)\quad g = a(5Z^2 + 5Z - 4)(1-Z)^{-7/8}\left(1+\tfrac{3}{5}Z\right)^{-9/8} C^{-3} \qquad \zeta = bZ(1-Z)^{-5/8}\left(1+\tfrac{3}{5}Z\right)^{-3/8} C^{-1} \quad \left(-\tfrac{5}{3} < Z < 1\right)$$

$$(3)\quad i > 0 \qquad \frac{d\tilde{u}_i}{d\zeta} = \phi_u^{(i)} \qquad \frac{d\tilde{v}_i}{d\zeta} = \phi_v^{(i)} \to \begin{cases} G_- & W_n = 0 \\ G_+ & (u,v) = P_{\varepsilon-M} \end{cases}$$

$$\tilde{u}_i = \tilde{u}_i^{(1)} + \tilde{u}_i^{(2)} \qquad \tilde{v}_i = \tilde{v}_i^{(1)} + \tilde{v}_i^{(2)}$$

$$(4)\quad \frac{d\tilde{u}_i^{(2)}}{d\zeta} = 0 \qquad \frac{d\tilde{v}_i^{(2)}}{d\zeta} = 0$$

$$\tilde{u}_i^{(2)} = \frac{d\phi_i}{d\zeta} \qquad \tilde{v}_i^{(2)} = \frac{7+i}{4}\phi_i - \frac{5}{4}\zeta\frac{d\phi_i}{d\zeta} \qquad (2)\to(4)\begin{cases} t_i = \phi_i(1-Z)^{(7+i)/8}\left(1+\tfrac{3}{5}Z\right)^{3(7+i)/8} \\ \xi = \tfrac{1}{2} - \tfrac{1}{4}\sqrt{\tfrac{3}{2}(1-Z)} \end{cases}$$

$$\boxed{\begin{array}{l} \xi(1-\xi)t_i'' + \frac{9+2i}{6}(1-2\xi)t_i' - \frac{(7+i)(9+i)}{3}t_i = 0 \\ t_i = [\xi(1-\xi)]^{\left(\frac{5}{2}+\frac{i}{3}\right)}\frac{d^{(7+i)}}{d\xi^{(7+i)}}[\xi(1-\xi)]^{\left(\frac{2i}{3}+\frac{9}{2}\right)} \\ \tilde{u}_i, \tilde{v}_i \to f(t_i) \;/\; i = 1,2,\ldots \end{array}} \qquad \boxed{i = 0,1,2}$$

FIGURE 2

The solution describing the plane and axisymmetric transsonic flow of a perfect gas in the vicinity of G has the form of a power series in n, (the distance is measured from the surface of the body, where $n = 0$) with coefficients depending on the corresponding self-similar variable ζ. The principal term of this expansion (for $i = 0$) corresponds to plane potential flow; the terms of the expansion for $i > 0$ (taking into account the axisymmetric and eddy character of the flow) are determined from a system of linear nonhomogeneous ordinary differential equations. By introducing a parametric representation for the function g, V. F. Shugayev succeeded in constructing an analytical solution which greatly simplified the introduction of asymptotic solutions into the numerical algorithm.

Outside the region G we use the algorithm in the usual form as given by Scheme II (the system of ordinary differential equations is integrated across the shock layer from the wave to the body). The additional conditions of matching of both solutions at the boundary of this region make the problem single-valued.

On the whole, we succeed in constructing numerical algorithms allowing us to find the solution with a high degree of accuracy. The solution outside the zone of influence of the blunt body was generally constructed by the method of characteristics. Some results of calculations obtained by A. Bulekbayev, V. F. Ivanov, E. S. Sedova, and F. V. Shugayev are given [2].

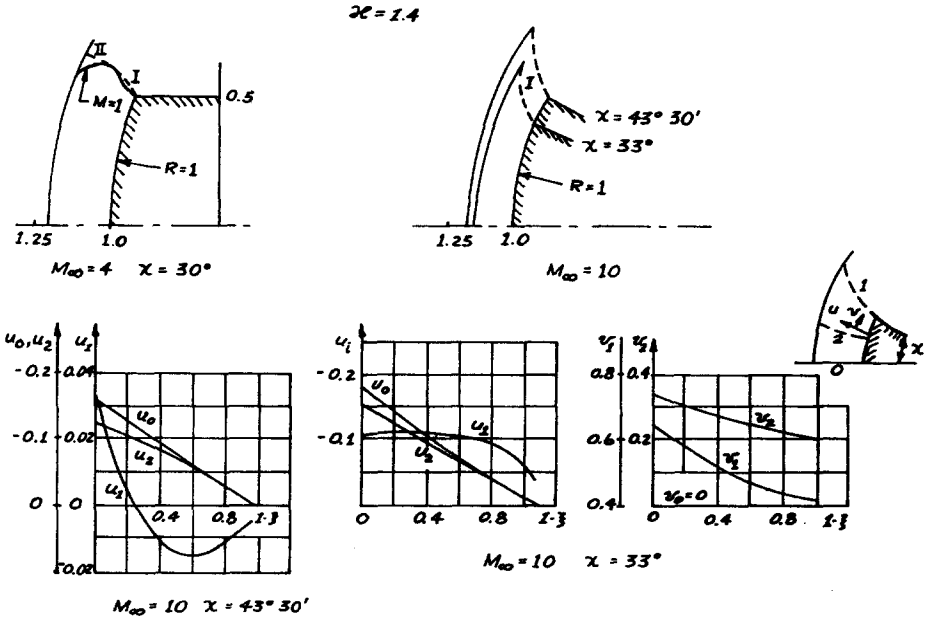

FIGURE 3

Figure 3 shows shock waves, sonic lines, and limiting characteristics for flow of a perfect gas ($\varkappa = 1.4$) around a spherical segement with a sonic discontinuity at the semiangle $\chi = 30°$ ($M_\infty = 4$), and $\chi = 33°$ and 43°30 ($M_\infty = 10$). The distribution of velocity components u^i, v^i (along n, S, respectively) along the axis of symmetry ($i = 0$), of the limiting characteristics ($i = 1$) and of the intermediate line ($i = 2$) are also given. It is seen that the behavior on the limiting characteristic strongly depends on the semiangle of the segment. The results of the flow calculations by this method with secondary shocks are given in Fig. 15.

3. *Calculation of Flow Around A Cylindrical Flat-Nose Body Under Transsonic and Supersonic Conditions*

Calculations of transsonic and supersonic flows around a cylindrical flat-nose body were carried out by means of the method of "large particles" [6–8]. The problem was chosen to make it possible to carry out the calculations for a whole spectrum of flow conditions ranging from purely subsonic flow to hypersonic flow (including transsonic regions and transitions through sonic velocity). The calculations were made by Iu. M. Davidov [8]. Here we did not single out the shocks in the flow beforehand. Such a "sweeping-through" method turned out to be reasonable, due to the presence of the lines of discontinuity within the disturbed region.

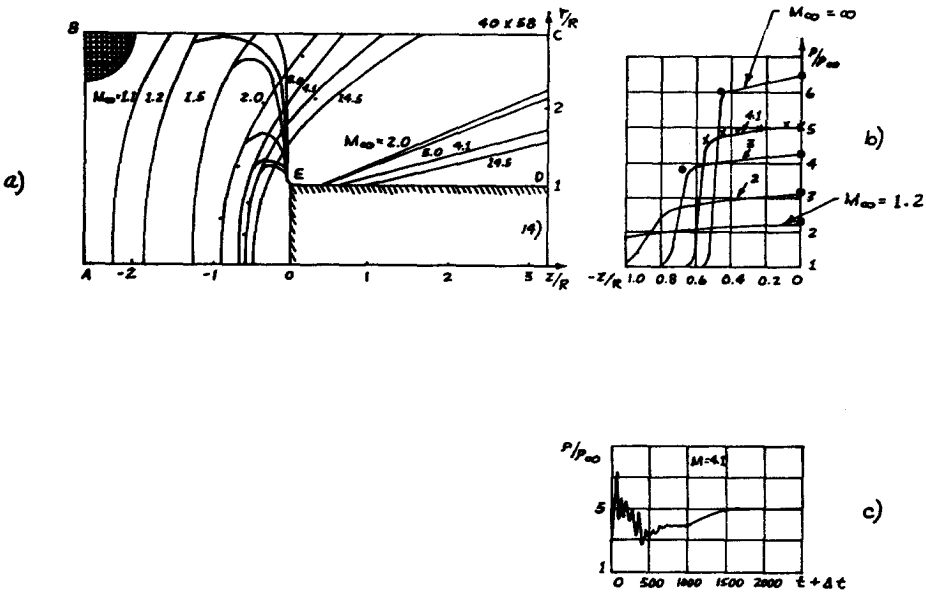

FIGURE 4

In Fig. 4 the positions of the nose and internal shock waves and the sonic lines for various Mach numbers of the undisturbed flow $1.1 \leqslant M_\infty \leqslant 14.5$ are given. For $M_\infty < 2$ the secondary shocks in the flow are not shown, due to their weak intensity (with increasing M_∞ the strengths of the internal shocks in the flow become greater). Shock waves are defined here as lines on which the density derivative with respect to one of space directions has a maximum.

In Fig. 4b the density distribution along the axis of symmetry of the body is given. Dotted lines show values of the density behind the direct shock in the flow and at the stagnation point. Discontinuities due to shocks are seen to be "smeared" over several cells in space, with the smearing band of the wave being wider, the smaller the values of Mach numbers M_∞. Crosses in Fig. 4b indicate the results of calculations by a characteristic network method. As should be expected, the corner point in such flows is a sonic discontinuity. No special expansions in its vicinity were carried out. Drawing sonic lines is of interest because here the regions of influence of the blunt body of II type are bounded "above" by characteristics of I and II families.

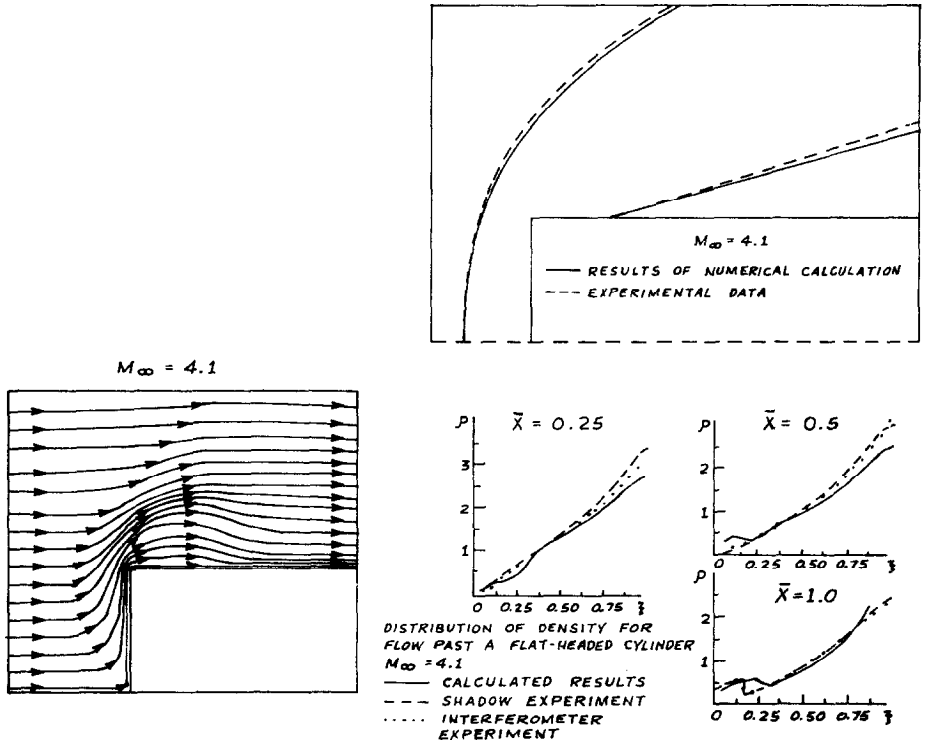

FIGURE 5

Figure 4c reveals the time history of the value of the density at the stagnation point of the body as it approaches the steady value.

In Fig. 5 ($M = 4.1$) the result of the numerical solution (solid lines) are compared with the results of experiment (dotted lines and dots). In the graphs the positions and forms of the nose and secondary shock waves and the density distribution at $\bar{X} = Z/(2R) = \text{const}$ are given (along the abscissa the coordinate

$$\zeta = (\tau - \tau_0)/(\tau_1 - \tau_0)$$

is plotted, where $\tau = \tau_0(Z)$ and $\tau = \tau_1(Z)$ are the equations of the body and shock wave, respectively. Experimental points are also plotted in Fig. 4a. The results are in fairly good agreement, especially in the flow field and on the shock wave.

In Fig. 6 are plotted the lines $M = \text{const}$ for the disturbed flow under transsonic conditions $0.6 \leqslant M_\infty \leqslant 1.2$ (the value of the critical Mach number is $M_{cr} = 0.7$).

To eliminate, if possible, the influence of the boundary conditions on the flow pattern, the calculation for "overcritical" velocities were carried out with different values of the ratio of the length l of the cylindrical flat-nosed body to its

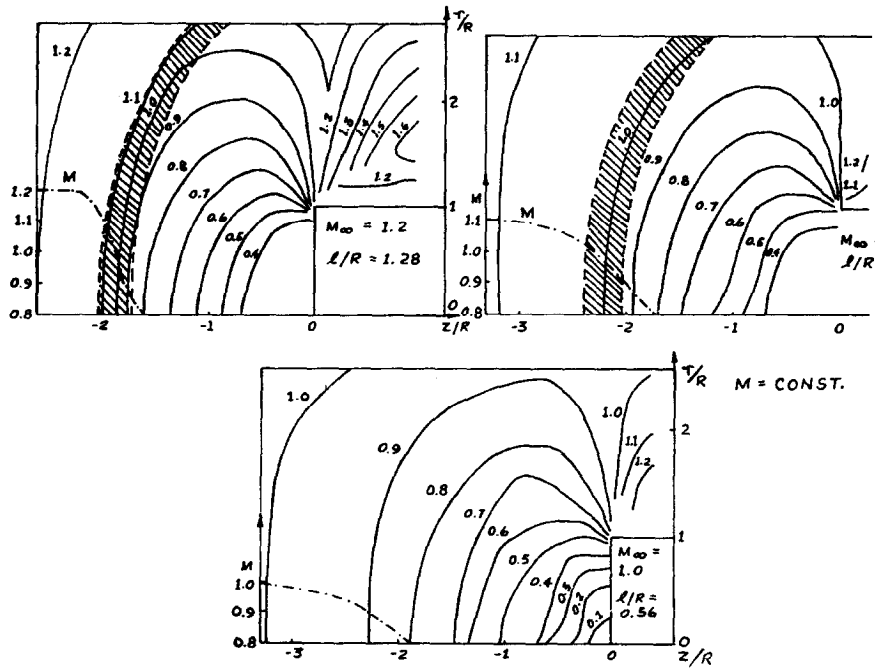

FIGURE 6

radius R. In Fig. 7 results of such calculation for $M_\infty = 0.9$ are shown. The field ahead of the body was determined rather quickly, and for the cases in question it practically remained unchanged at distances up to $1.5R$. The flow to the right of the cut is stabilized for $l/R \sim 2$. Boundary conditions at the left limit become important as the end is moved out farther. It is desirable in the future to use a finer calculation network.

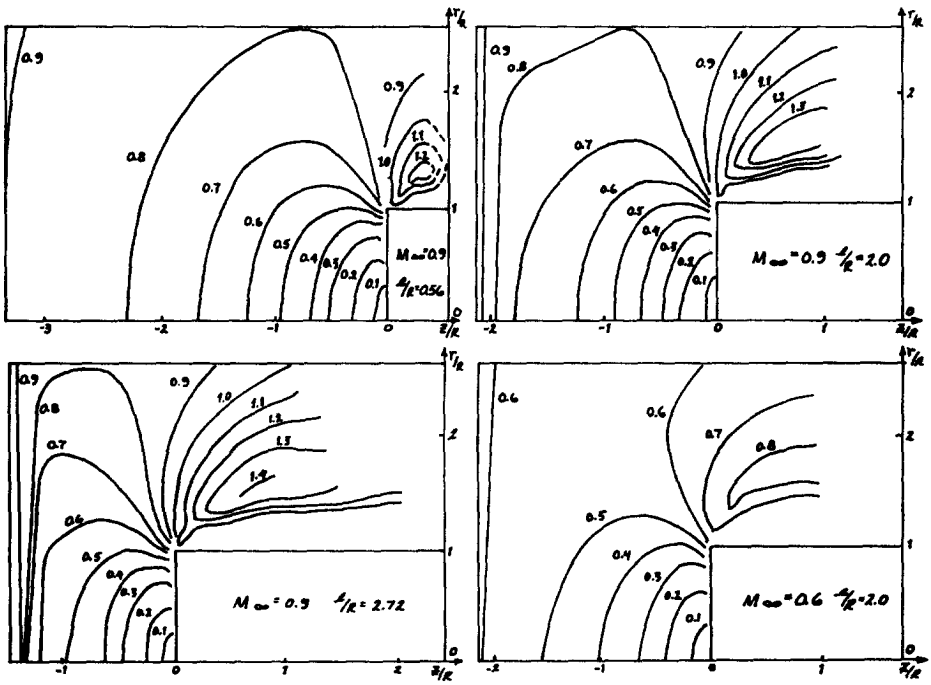

FIGURE 7

4. *Three-Dimensional Flows*

In this section we give a scheme for constructing a characteristic network method developed by K. M. Magomedov and A. S. Kholodov [5]. Consider the system of quasilinear partial differential equations of hyperbolic type of the first order in the general form

$$\bar{v}_t + A\bar{v}_x + B\bar{v}_y + \cdots = \bar{f}, \tag{1}$$

where the matrices A and B, the column vector on the right-hand sides, $\bar{f}$, and the vector function, v, may be functions of t, x, y,..., the unknown variables with N components. We shall further restrict consideration to the three-dimensional case, as the extension of the method to a greater number of variables is formal.

Suppose that the matrices A and B have only real eigenvalues (there may be some values which are equal). Let μ_i and $\bar{\omega}_i$ $(i = 1, 2,..., N)$ be eigenvalues and eigenvectors, respectively, of the matrix A', and μ_i and $\bar{\omega}_i$ $(i = N + 1,..., 2N)$ of matrix B'. Then Eq. (1) may be reduced to one of the following characteristic (normal) forms

$$\begin{aligned} \bar{\omega}_i \bar{v}_{ti} &= \bar{\omega}_i \bar{f} - \bar{\omega}_i (B\bar{v}_y), \qquad i = 1, 2,..., N; \\ \bar{\omega}_i \bar{v}_{ti} &= \bar{\omega}_i \bar{f} - \bar{\omega}_i (A\bar{v}_x), \qquad i = N + 1,..., 2N. \end{aligned} \tag{2}$$

Here $\bar{v}_{ti} = \bar{v}_t + \mu_i \bar{v}_x$, $(i = 1, 2,..., N)$ and $\bar{v}_{ti} = \bar{v}_t + \mu_i \bar{v}_y$, $(i = N + 1,..., 2N)$, are derivatives along two-dimensional characteristics on the surfaces $y = \text{const}$ and $x = \text{const}$, respectively, or in other words, along the lines of intersection of characteristic and coordinate surfaces.

Consider now the $3N$ Eqs. (1) and (2). It is obvious that the number of independent variables among them is equal to N. We can use this fact to construct explicit difference schemes not requiring, for example, any approximation of partial derivatives with respect to x and y. If we know the solution on the layer

$$\begin{aligned} \bar{v}(H) - \bar{v}_0 + \tau\nu(A\bar{v}_x + B\bar{v}_y - \bar{f})_0 + \tau(1 - \nu)(A\bar{v}_x + B\bar{v}_y - \bar{f})_H \\ = 0[(1 - 2\nu)\tau^2 + \tau^3], \\ \bar{\omega}_i(\bar{v}_{tH} - \bar{v}_i) + \tau\nu\bar{\omega}_i(B\bar{v}_y - \bar{f})_i + \tau(1 - \nu)\,\bar{\omega}_i(B\bar{v}_y - \bar{f})_H \\ = 0[(1 - 2\nu)\tau^2 + \tau^3], \qquad \tau = 1, 2,..., N \qquad \text{etc.} \end{aligned} \tag{3}$$

Equations (3) contain $3N$ unknowns $\bar{v}(H)$, $\bar{v}_x(H)$, $\bar{v}_y(H)$ and the same number of equations. We can show that by elimination of $\bar{v}_x(H)$, $\bar{v}_y(H)$ from this system we have the difference equations approximating Eq. (1):

$$\begin{aligned} \bar{v}(H) = \bar{F}[t_0, x, y, \bar{v}(t_0, x, y), \bar{v}(H), \nu\tau\bar{v}_x(t_0, x, y), \nu\tau\bar{v}_y(t_0, x, y)] \\ + O[(1 - 2\nu)\tau^2 + \tau^3]. \end{aligned} \tag{4}$$

In deriving this relation finite-difference relations simply replace ordinary derivatives along certain lines. The conservation in the difference equations of partial derivatives with respect to x and y on the layer $t = t_0$ depend, as is seen from Eq. (3), on the choice of ν. If $\nu = 1/2$ the Eqs. (4) will be correct to the second order of approximation with respect to t, and, generally speaking, contain $\bar{v}_x(t_0)$, $\bar{v}_y(t_0)$. If $\nu = 0$ (the first order approximation with respect to t) these derivatives are dropped.

By transforming the region in which the solution is constructed to rectangular

form, by introducing the fixed network $t = n\tau$ ($n = 0, 1, 2,...$), $x = mh_1$, $y = lh_2$ ($m, l = 0, 1, 2,...$), and denoting the values of functions at the nodes of the network by $\bar{v}^n_{m,l}$ and, furthermore, given the relation of the parameters with indices 0 and i ($i = 1, 2,..., 2N$) with known values of $\bar{v}^n_{m,l}$ on each layer $t = t_n = n\tau$, we arrive at the ordinary difference scheme with fixed network or the method of networks

$$\bar{v}^{n+1}_{m,l} = \sum_{i,j} c_{i,j}\bar{v}^n_{m+i,l+j} + \tau\bar{\Phi}(t_n, t_n + \tau) \tag{5}$$

where c_{ij} are matrices whose elements for the schemes of first order depend only on the parameters for $t = t_n$ and in the second order schemes for quasilinear equations also on $\bar{v}^{n+1}_{m,l}$.

Unlike the existing formulations of the method of characteristics, the approach given above is related formally neither with the dimensions of the space considered nor with the concrete form of the equations and makes use of a convenient fixed network. Further, by suitable choice of ν and order of interpolation in the same computer program, we can obtain schemes of different order of approximation. For linear interpolation we take $\nu = 0$ (Scheme I), for the quadratic case $\nu = 1/2$ (Scheme II). Thus we have the schemes of first or second order accuracy for all variables. Note that in the one-dimensional case ($B = 0$) and with linear interpolation the scheme represented by Eq. (5) coincides with the method proposed by Courant, Isaacson, and Rees [12].

The main properties of the above schemes (stability, monotonic behavior, magnification of possible errors, etc.) as related to convergence, were studied analytically [5] by means of linear model equation and verified in practice by a series of problems of gas dynamics. For the case of the equation of gas dynamics, the difference scheme is given in [5].

By means of the nonsteady characteristic network method described above, A. S. Kholodov carried out detailed investigation of the properties of three-dimensional supersonic flow around bodies of different shape. Calculations were made by a single algorithm throughout the whole region of disturbance without separating out any singularities beforehand. Bodies of complex form were considered (segements with sharp corners, inverted cones, etc.) in the presence of chemical reactions in the gas and angles of attack up to $\alpha = 25$–$30°$.

Some remarks should be made about the formulation of the problem. The solution is given in the region $ABCD$ (Fig. 8) bounded by the initially unknown shock wave AB, by the axis of symmetry of the flow AD, by the body CD, and by some ray BC. The boundary conditions are: on the shock wave the Rankine–Hugoniot relations, on AD—the condition of symmetry of the flow, on the body—the conditions of nonpenetration.

If the ray BC is completely situated in the supersonic region of the flow, the

parameters on it are calculated as within *ABCD* (the Mach cone is situated within the region). As initial data the shock wave surface was given (paraboloid, for example), also a linear distribution of velocity on the body and a linear distribution of parameters between the body and the wave was used.

The region *ABCD* was covered with a uniform network at the nodes of which the parameters were calculated on layers $t = \text{const}$ until a stationary pattern of flow was attained. For calculating axisymmetrical flows a network was used consisting of 21 points on the body and 11 points across the shock layer (some cases were calculated by means of a 41×21 network). The data at angle of attack were obtained essentially by a $11 \times 6 \times 11$ network (6 points across the shock layer with quadratic interpolation.)

In Fig. 8 the flow pattern (Fig. 8a) and surface pressure distribution for supersonic flow of a sphere-cone body at a zero angle of attack and at various Mach numbers in the undisturbed air stream ($æ = 1.4$) are given. In Fig. 8a the geometry of the body, the position of detached shock waves and sonic lines with

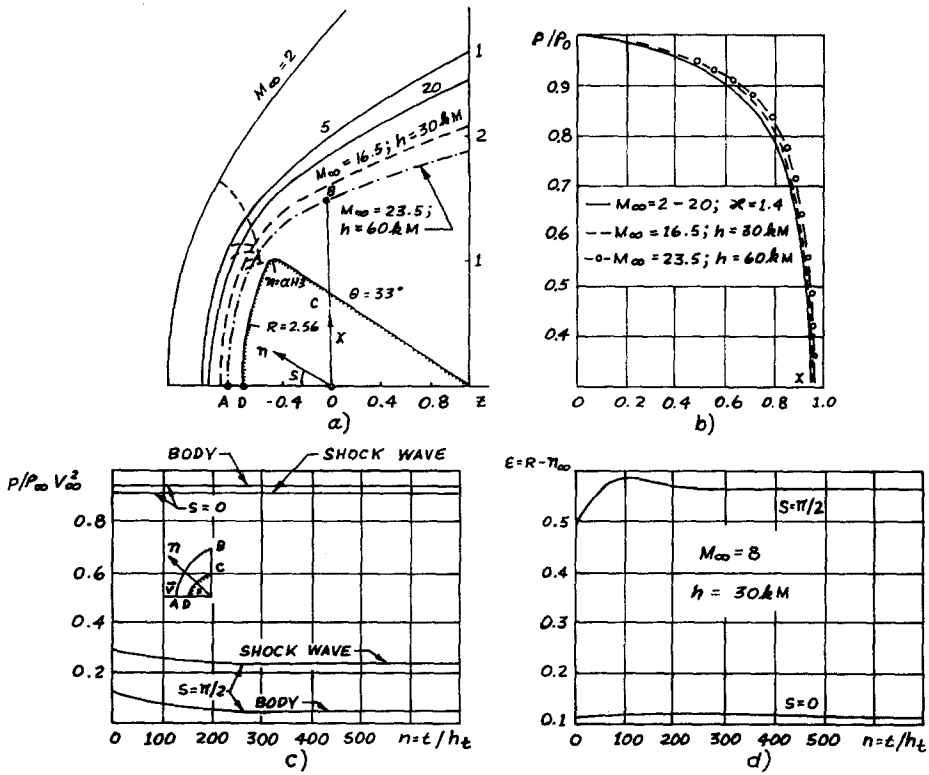

FIGURE 8

Mach numbers from $M_\infty = 2$ to $M_\infty = 23.5$ are represented. In the case $M_\infty = 16.4$ (height $h = 30$ km) and $M_\infty = 23.5$; ($h = 60$ km) chemical reactions were taken into account. In Fig. 8b for the same Mach numbers the pressure distribution along the body, expressed as a ratio to the stagnation pressure (solid lines, $M_\infty = 2,\ 5,\ 20$; $æ = 1.4 = \text{const}$, dotted lines—chemical transformations included) is given. It is seen that if $æ = \text{const}$ all curves coincide. In the presence of chemical reactions (when the effective $æ$ decreases) the profile of the pressure distribution becomes more "complete" with increasing M_∞.

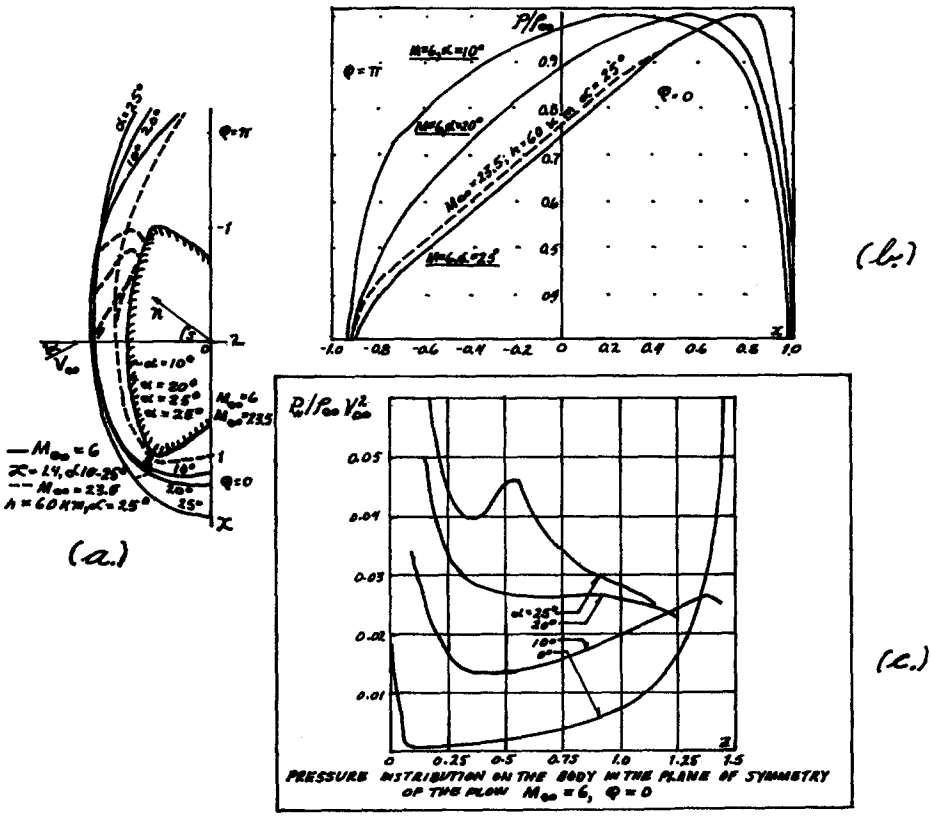

FIGURE 9

In Fig. 9 some results for the same body moving at an angle of attack $\alpha = 10°, 20°, 25°$ for Mach number $M_\infty = 6$ are given. The case when $M_\infty = 23.5$ ($h = 60$ km), $\alpha = 25°$ is also considered with account taken of equilibrium chemical reactions. In Fig. 9a the position of the detached shock waves, the sonic lines and the stagnation points (constructed from the velocity distribution)

in the plane of symmetry of the flow are given. For these flow conditions there is also given the distribution of pressure (in terms of the maximum pressure) on the surface of the body along the nose part $\varphi = 0, \pi$ (Fig. 9b) and in the plane of symmetry $\varphi = 0$ (Fig. 9c). In the latter case sharp nonmonotonic behavior at large angles of attack is observed. We note that the point on the body where the pressure is maximum does not coincide with the stagnation point, determined from the velocity distribution.

The approach of parameters to a steady state is shown in Fig. 8. The establishment of steady state pressure (Fig. 8c) for the flow with chemical reactions past a sphere for $M_\infty = 8$, $h = 30$ km is given (at points A, B, C, D). Figure 8d shows the establishment of the shock wave at points A and B. It is seen that the number of time steps necessary for the attainment of steady state is of the order of 300–400.

By means of a characteristic network method complex calculations of long bodies of complicated configuration were also made. Figure 10 shows the flow pattern around a cylinder with a spherical nose and conical afterbody for $M_\infty = 6$, $\alpha = 10°$, where we can see explicitly the zone of interaction of the internal shock

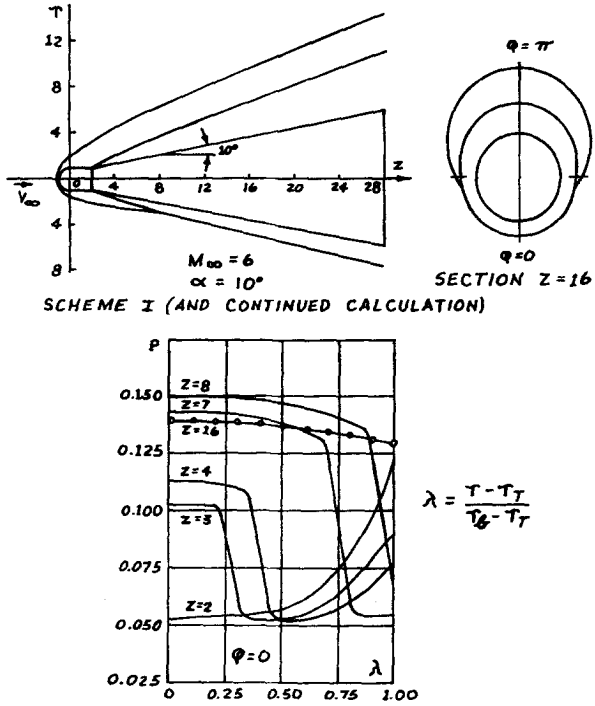

FIGURE 10

with the main one. Also the profiles of pressure (in the plane $\varphi = 0$) across the shock layer in different sections $z = \text{const}$ are given. The internal shock is seen to be "smeared" over 2–3 steps with respect to λ, ($h_\lambda = 0.05$) though in Fig. 10 it is conventionally plotted as a line. The coordinate $\lambda = (\tau - \tau_0)/(\tau_1 - \tau_0)$, where $\tau = \tau_0(z, \varphi)$ and $\tau = \tau_1(z, \varphi)$ are the equations of the body and nose shock wave, respectively.

5. *Secondary Shocks in the Flow*

Under some conditions of supersonic flow around blunt bodies (cones, wedges, etc.), in the flow field behind the detached shock wave, secondary "floating" shocks occur (n.s.f.) which greatly affect the aerodynamic characteristics of the vehicles. Such phenomena were first discovered by means of calculations [3] and confirmed afterwards as a result of experiments. The origin of formation of "floating" shocks in the flow, the conditions under which they occur (configuration of the bodies, conditions of flight, etc.) and also properties of such flows are at present insufficiently studied.

Here we shall give some results of calculations related to the formation of "floating" shocks in the flow. Calculations were carried out by the above methods for an ideal gas for smooth blunt bodies as well as for bodies with sonic and supersonic corners on the contour.

Let us dwell on the properties of flow which result in the formation of "floating" shocks in the flow. When flowing around blunt cones or wedges, a sudden stagnation of the flow occurs when changing from the blunt to the rectilinear part of the contour. This induces a convergence of characteristics and the formation of compressions emanating from the surface of the body behind the junction point of the contours. In those cases when the gradient of pressure behind the characteristic, bounding the region of influence of the blunt body is large, and the shock layer is sufficiently wide, the compressions develop into a shock wave situation within the flow having zero intensity at the initial moment.

All the cases of "spontaneous" generation of shock waves are related to the phenomenon of intersection of the characteristics of the same family. In such flows where there occurs a whole region which is covered twice by the characteristics of one family, a new shock wave emanates from the cusp A of the envelope of these characteristics. The cusp itself does not initially develop a discontinuity, however the derivatives of velocity, density, pressure, etc. become infinite there, and for this reason the intensity of the "floating" shock in the flow is equal to zero and later a "real" shock wave appears.

In practice we have no need to define exactly the position of the node point in the formation of a "floating" shock in the flow from zero intensity. The shock wave originates from the point at which characteristics of the same family, as

calculated, will cross. We note that "floating" shocks in the flow, due to their comparatively weak intensity, may be accurately constructed only by means of the direct scheme of the method of characteristics.

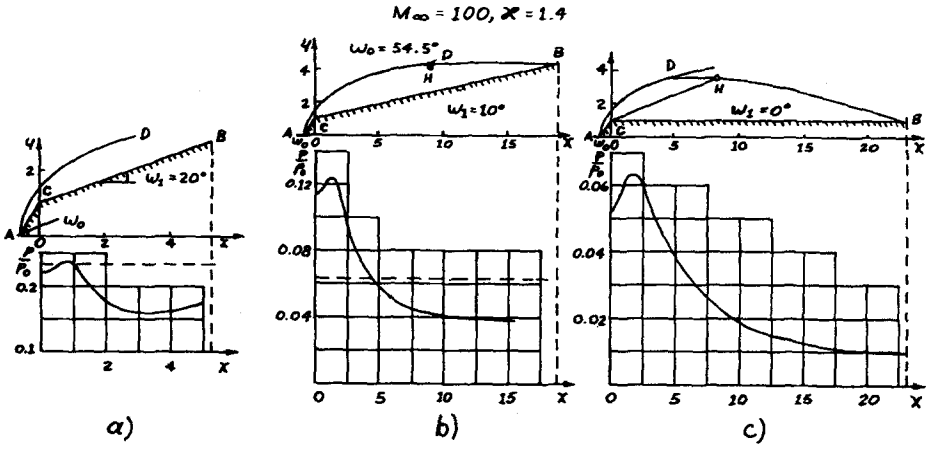

FIGURE 11

In Fig. 11 examples are given of calculations of flow taken from paper [10] at $M_\infty = 100$; $æ = 1.4$ for flow past frustrums of cones (semiangle $\omega_1 = 20°$—Fig. 11a; $\omega_1 = 10°$—Fig. 11b; $\omega_1 = 0$—Fig. 11c) with a common conical head section ($\omega_0 = 54.5°$). The broken line ACB is the generator of the body of revolution; AD is the shock wave and BD the characteristic of the second family on which the intersection of characteristics of the first family occurs. The region of intersection of characteristics (if any) is indicated by a circle with letter H. In Fig. 11c the line CH is the last characteristic of the fan originating at the point C. In Fig. 11a and Fig. 11b the pressure on sharp cones with semiangles 20° and 10°, respectively, and for the same M_∞ are plotted by chain-dotted lines. Linear dimensions are expressed in terms of the radius at the junction point of the cones. The pressure is given as a ratio to the stagnation pressure.

As is seen from the graphs, in the third case the "floating" shock originates inside the flow field, in the second case it develops immediately behind the nose shock wave; on the other hand, in the first example the "floating" shock does not occur at all in the shock layer. In addition, it should be noted that the pressure gradient at the junction point increases as the semiangle of the frustrum of the cone decreases, and the shock layer becomes relatively thicker.

The calculations were confined to an ideal gas. Initial conditions for the method of characteristics were obtained from the exact solution for the sharp cone, which provided high accuracy for the calculations. These examples show that properties

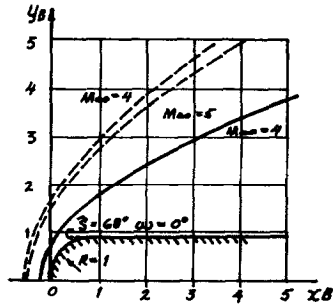

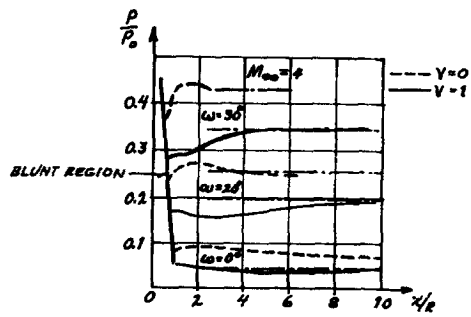

FIGURE 13

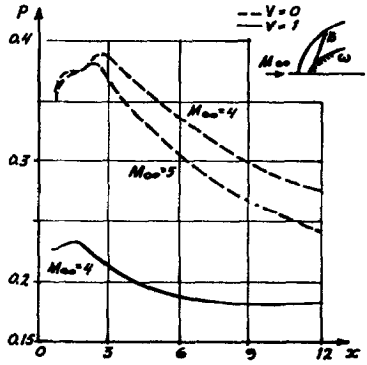

FIGURE 12

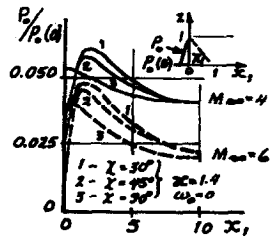

FIGURE 14

of the flow depending on viscosity (i.e., the separation of the boundary layer) are not responsible for the phenomenon of formation of a "floating" shock in the flow. The fact of their appearance is not connected with using "rough" initial data in the numerical solution of the supersonic region by the method of characteristics. Thus, the conditions of flow of blunt cones and wedges, leading to the formation of a positive pressure gradient behind the junction point of the contours, and the rather wide shock layer cause the formation of the "floating" shock in flow. Its position is defined by the intersection of two neighboring characteristics of the same (the first) family. Let us illustrate this by different examples.

Figure 12 gives shock waves and the distribution of pressure along the body for plane ($\nu = 0$) and axisymmetric ($\nu = 1$) bodies of a particular form (blunt spherical segment, discontinuity of slope, $\chi = 68°$, $\omega = 0$). Fig. 13 gives the pressure profile along smooth spherical cones (solid line) and wedges (dotted line) for different cone angles [3].

It follows that, other conditions being equal (free stream conditions, shape of the contour, etc.), the plane blunt body, in comparison with the axisymmetric

body (or the body with sonic discontinuity in comparison with the smooth body) introduces a larger disturbance into the supersonic flow. For this reason the shock layer here is thicker. In addition, for blunt slabs $\omega = 0$ and wedges $\omega \neq 0$ (plane flows) as well as for bodies with a sonic discontinuity (Fig. 14) a zone of over-expansion is formed immediately beyond the blunt section. At the point of junction of the blunt section with the rectilinear section a positive pressure gradient occurs in all cases, and thus sharply increases with increase of ω.

Hence, other conditions being equal, conditions for the development of "floating" shocks are more favorable in the plane case or for bodies with a sonic discontinuity.

In Fig. 15 nose shock waves and a "floating" shock in the flow are drawn. They arise in the supersonic zone in the flow around cones with blunt segments and a sonic discontinuity ($\chi = 30°$; $æ = 1.4$) [2]. Cones with different semiangles ($\omega = -5°$, $0°$, $10°$) and Mach number of oncoming flow $M_\infty = 4$ (solid line) and $M_\infty = 6$ (dotted line) are considered. The intensity of the "floating" shock at first rapidly increases, and then gradually decreases with distance from the blunt section. In some cases the maximum deflection angle of the flow on passing

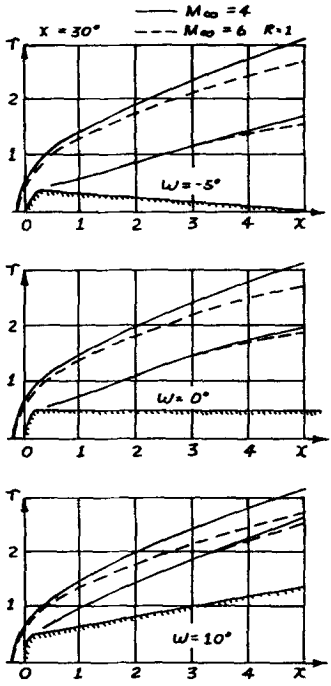

FIGURE 15

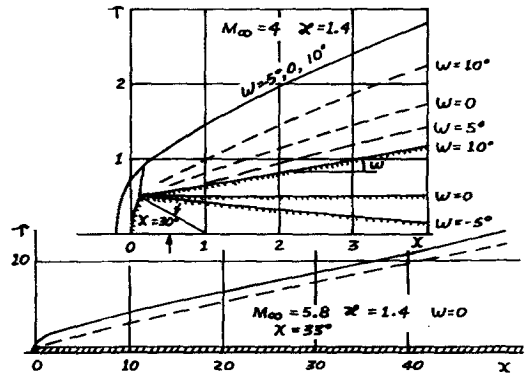

FIGURE 16

through the "floating" shock reaches several degrees, but at the distance of 30–40 radii of the blunt section the angle of rotation of the flow reaches only several seconds. V. F. Ivanov is the first who made a table of position of "floating" shocks [2]. We note that in the above cases, in the presence of "floating" shocks, the forms and positions of nose shock waves (in the region before the intersection with the "floating" shock) coincide (at the same values of Mach numbers of oncoming flow) for different semi-cone angles, $-10° \leqslant \omega \leqslant 10°$ (Fig. 16). The above property is apparently explained by the considerable region of influence of the blunt section, which for such conditions of flow, extends over a comparatively large region of the nose shock wave.

Figure 17 illustrates the influence of the point of discontinuity on the position of the limiting characteristics. An analogous phenomenon concerning the region of influence is observed for smooth blunt cones.

Figure 18 shows the coordinates of the shock wave for smooth cones with blunt noses. The coordinates point B at different ω are plotted where the characteristic limiting the region of influence of the blunt body occurs.

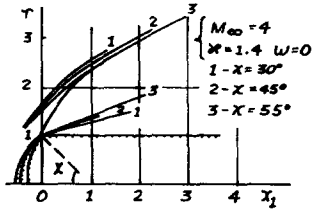

FIGURE 17

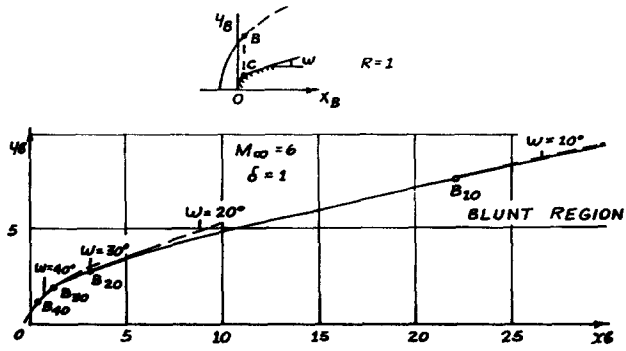

FIGURE 18

Figure 19 gives examples of flow obtained by V. J. Kosarev with "floating" shocks for flow around an axisymmetric body at $\alpha = 0$ and $5°$ ($\varkappa = 1.4$; $M_\infty = 6$) involving isentropic compression of the flow (smoothly joined cones: nose cone $\omega_0 = 10°$ and tail cone $\omega_1 = 20°$). In the figure is given the flow pattern (the "floating" shock in the flow is marked by a chain-dotted line) and the distribution of pressure along the surface of the body in the planes $\varphi = 0$, $\pi/2$, π. In the presence of a rather wide shock layer and a positive gradient of pressure, the formation of a "floating" shock in the flow ($\alpha = 0°$; $\alpha = 5°$, for $\phi = 0$, $\pi/2$) is explicitly seen.

The results of analytical investigations of the problems of the formation of a "floating" shock in the flow will now be given. The existence of such shocks in the flow in the case of the plane slab with a wedge head was proved first by A. A. Nikolski under the assumption of constant entropy. E. G. Shifrin [11] considered the conditions of formation of secondary waves for plane rotational flows. Let us dwell on the results of this work.

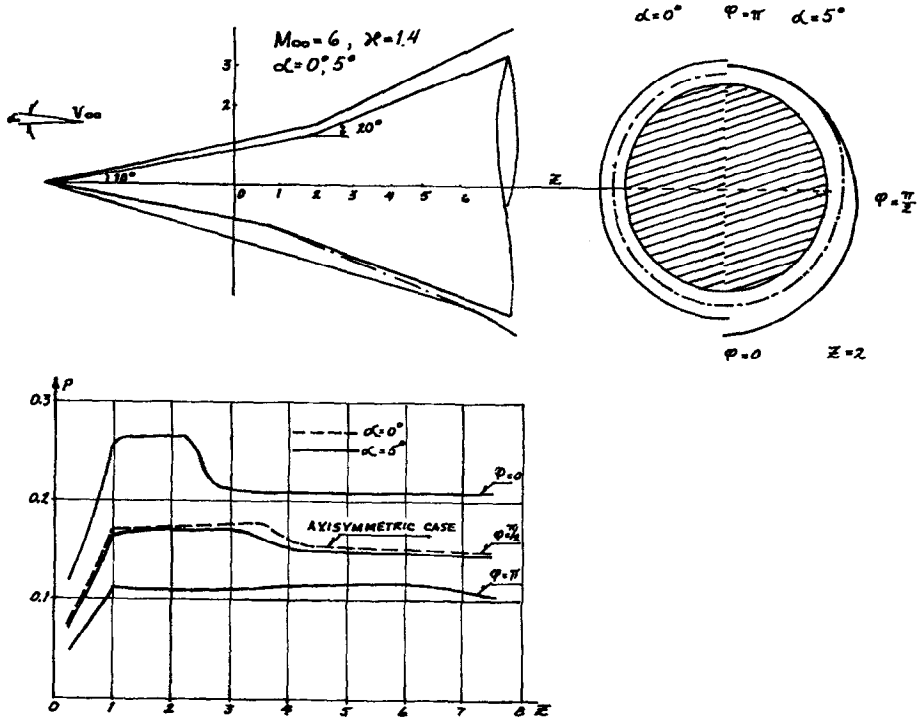

FIGURE 19

We succeeded in suggesting some reasons for the formation of "secondary" shocks for flow around a convex profile with a detached shock wave. We supposed that such a profile exists when the flow behind the shock wave is continuous and in the minimum region of influence, and when the entropy is a monotonically decreasing function of the stream function (shock is convex). The condition of breakdown of continuous supersonic flow in the characteristic triangle ABC determined by the profile and the adjoining minimum region of influence (Fig. 20)

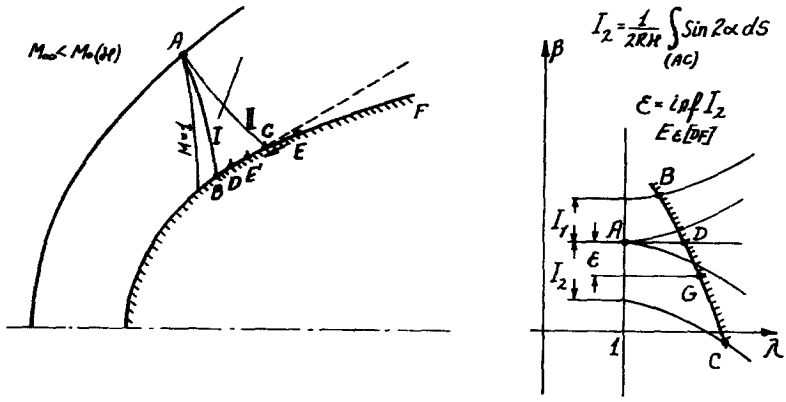

FIGURE 20

was found, namely: "If we subject the profile to continuous deformation, replacing part of its contour (downstream from some point E) by the tangent to the profile at this point, and then move it upstream, then the point E hardly manages to reach the minimum region of influence as continuous supersonic flow in the maximum characteristic triangle adjacent to the minimum region of influence is destroyed."

It is shown that, if in the flow past an infinite blunt wedge with a detached shock wave, we gradually increase the angle of the opening, while keeping the flow behind the shock wave at infinity supersonic at all times, either a shock or a local subsonic zone of isentropically stagnated gas will occur in the flow (Fig. 20). An analogous result is found in the flow around a profile with a discontinuity of contour slope, the point of origin of the sonic line.

REFERENCES

1. O. M. BELOTSERKOVSKII, A. BULEKBAYEV, AND V. G. GRUDNITSKII, Algorithms for schemes of the method of integral relations applied to the calculations of mixed gas flows, *Zh. Vychisl. Mat. Mat. Fiz.* 6, 6 (1966), 1064–1081.

2. O. M. BELOTSERKOVSKII, A. BULEKBAYEV, M. M. GOLOMAZOV, V. G. GRUDNITSKII, V. K. LUSKIN, V. F. IVANOV, Y. P. LUN'KIN, F. D. POPOV, G. M. RYABINKOV, T. Y. TIMOFEEVA, A. I. TOLSTIKH, V. N. FOMIN, AND F. V. SHUGAYEV, Flow past blunt bodies in supersonic flow: theoretical and experimental results, (O. M. Belotserkovskii, ed.), *Trady Vych. Tsentr. AN SSSR*, published by Computing Center, ANSSSR, 1st edition, 1966; (2nd edition, revised and extended), 1967, (NASA TT, F–453, 1967).
3. P. I. CHUSHKIN, Blunt bodies of simple form in supersonic gas flow, *P.M.M.* 5, **24** (1960), 927–930.
4. P. I. CHUSHKIN, Method of characteristics for three-dimensional supersonic flow, *Trady Vych. Tsentr. AN SSSR*, Moscow, 1968.
5. K. M. MAGOMEDOV AND A. S. KHOLODOV, On the construction of difference schemes for equations of hyperbolic type based on characteristic coordinates, *Zh. Vychisl. Mat. Mat. Fiz.* 2, **9** (1969), 373–386.
6. F. H. HARLOW, The Particle-in-Cell Computing Method for Fluid Dynamics—Methods in Computational Physics," Vol. 3, (Berni Alder, Sidney Fernbach, Manuel Rotenberg, eds.,) Academic Press, New York, 1964.
7. MARVIN RICH, A method for Eulerian fluid dynamics, Los Alamos Scientific Laboratory, New Mexico, Lab. Rep. LAMS-2826, 1963.
8. O. M. BELOTSERKOVSKII AND Y. M. DAVIDOV, Unsteady method of large particles for problems of external aerodynamics (In press.).
9. P. I. CHUSHKIN, Calculations of certain sonic gas flows, *P.M.M.* 3, **21** (1957), 353–360.
10. O. N. KATSKOVA, I. N. NAUMOVA, Y. D. SHMYGLEVSKII, AND N. P. SHULISHNINA, Attempt to calculate plane and axisymmetric supersonic flows of a gas by the method of characteristics, published by Computing Center, AN SSSR, Moscow, 1961.
11. E. G. SHIFRIN, On one-condition for breakdown of regions of continuous supersonic flow for flow past profiles with detached shock waves, *Dokl. Akad. Nauk. SSSR*, 4, **176** (1967), 797–800.
12. R. COURANT, E. ISAACSON, AND M. REES, *Comm. Pure Appl. Math.* **5** (1952), 243.